Plastic response of a 2d amorphous solid to quasi-static shear : I - Transverse particle diffusion and phenomenology of dissipative events

Anaël Lemaître[(1)] and Christiane Caroli[(2)]

[(1)] *Institut Navier– LMSGC, 2 allée Képler,*
77420 Champs-sur-Marne, France and

[(2)] *INSP, Université Pierre et Marie Curie-Paris 6, CNRS,*
UMR 7588, 140 rue de Lourmel, 75015 Paris, France

(Dated: February 1, 2008)

Abstract

We perform extensive simulations of a $2D$ LJ glass subjected to quasi-static shear deformation at $T = 0$. We analyze the distribution of non-affine displacements in terms of contributions of plastic, irreversible events, and elastic, reversible motions. From this, we extract information about correlations between plastic events and about the elastic non-affine noise. Moreover, we find that non-affine motion is essentially diffusive, with a clearly size-dependent diffusion constant. These results, supplemented by close inspection of the evolving patterns of the non-affine tangent displacement field, lead us to propose a phenomenology of plasticity in such amorphous media. It can be schematized in terms of elastic loading and irreversible flips of small, randomly located shear transformation zones, elastically coupled via their quadrupolar fields.

I. INTRODUCTION

Plastic deformation of amorphous solids and, more generally, of jammed disordered media (foams, confined granular media, colloidal glasses,...) has been intensively studied in the past two decades. General agreement is now gradually emerging about the nature of the elementary dissipative events in these highly multistable systems. They consist in sudden rearrangements of small clusters comprising a few basic structural units, such as T_1 events in dry foams. In the case of glasses, where they cannot be observed directly, progress has come, following the pioneer work of Argon and collaborators, from extensive numerical studies [1, 2, 3]. More recently, simulations performed on model systems – Lennard-Jones (LJ) glasses – have proved very helpful to improve our understanding of the effect of topological disorder on the elastic as well as plastic shear response of amorphous solids.

MD simulations are instrumental in elucidating the thermal dependence of the flow stress $\sigma(\dot{\gamma})$ in the high strain rate ($\dot{\gamma} >> 1$) regime. However, such conditions (finite T, high $\dot{\gamma}$) "blur" the microscopic motion, making it difficult to characterize precisely the elementary events, which are the building blocks on which constitutive laws should be based. For this purpose, a second class of numerical works have focussed on the athermal ($T = 0$), quasi-static ($\dot{\gamma} \to 0$) regime. In this later regime, hereafter abbreviated as AQS, when a sample is sheared at constant rate, the stress-strain $\sigma(\gamma)$ curve exhibits (see Figure 1) elastic branches interrupted by discontinuous drops $\Delta\sigma$ which are the signature of the dissipative events. Beyond an initial transient, $\sigma(\gamma)$ fluctuates about an average value $\bar{\sigma}$, which is identified with the yield stress $\sigma_Y = \lim_{\dot{\gamma}\to 0} \bar{\sigma}(\dot{\gamma})$. The distribution of stress drops is broad and system-size dependent. In their study on a 2D LJ glass, Maloney and Lemaitre [4] were able to analyze them in terms of cascades of elementary events, which we will term "flips". Each such flip involves both the strong rearrangement of a small cluster ($\sim$ a few atoms), and the appearance of an associated quadrupolar elastic field. This result substantiates the representation of elementary processes as Eshelby-like [6] shear transformations [7].

However, it appears desirable to analyze AQS simulations in more detail, in order to shed light upon debated questions concerning phenomenologies based on the notion of shear transformation zones (STZ) [3, 8, 9]. Namely:

– Can the flipping clusters be associated with regions of the disordered solid which retain their identity over a finite range of elastic loading before they reach their instability

threshold?

– If so, do the simulations give information about the response of a zone to the elastic field generated by the flip of another zone?

– Can one evaluate the relative importance of the dynamic noise resulting from this mechanism as compared with disorder-induced fluctuations of the non-affine elastic field?

In order to address these issues, we extend in this article a recent study on a 2D LJ glass [10], by Tanguy et al, which confirms that plastic flow is spatially heterogeneous. They claim that one should distinguish between two types of plastic events: strongly localized ones occurring during the initial loading phase ($\sigma << \sigma_Y$), and non-localized ones which they term "non-permanent shear bands". They also investigate atomic motion in the direction transverse to the plastic flow. While they find it to be diffusive at long times, they conclude to its hyperdiffusive nature on short time intervals.

Transverse displacements are purely non-affine and, as indicated by the jagged shape of the $\sigma(\gamma)$ curve, consist of a succession of possibly noisy elastic episodes interspersed with sudden atomic rearrangements associated with the plastic events, hence the interest of a detailed analysis of their dynamics. With this remark in mind, we revisit in Section II the analysis of transverse particle motion, now explicitly separating elastic and plastic contributions. We thus extract information about *(i)* correlations between plastic events *(ii)* the elastic contribution to the non-affine noise invoked in the phenomenological STZ model of Falk and Langer [9]. Moreover, we find it inappropriate to qualify global transverse particle motion as hyperdiffusive at short times. Indeed, the effective diffusion coefficient $D(\Delta\gamma) = \langle\Delta y^2\rangle/\Delta\gamma$ smoothly increases with $\Delta\gamma$ from a *finite* short time value D_0 to the asymptotic value D_∞. Noticeably, the whole $D(\Delta\gamma)$ curve is *system size dependent* – a result which appears consistent with the analysis of plastic events in terms of flip cascades. We also show that the contribution of plastic events to transverse diffusion dominates markedly over the effect of disorder-induced non-affine elastic fluctuations.

In Section III, on the basis of close inspection of the evolution of the spatial structure of the infinitesimal non-affine field, we show that our results can be interpreted in terms of the elastic loading of zones driven by shear, which soften gradually as they approach their spinodal limit. As they approach this threshold, these zones give rise to quadrupolar fields of growing amplitude. The zones thus identified can be traced back over shear intervals substantially larger than the average interval between plastic events, the effect of which is

thus easily observable.

These observations support a description in terms of elastically loaded zones, and point towards the relevance of the dynamical noise generated by plastic flips themselves. The associated inter-zone elastic couplings should be responsible for the "autocatalytic avalanches" [5, 12] or flip cascades [4, 13] constituting the system-size dependent plastic events, which we believe to be precisely the non-permanent shear bands invoked in ref.[10]. We attribute the stronger localization of initial events to the smaller density of nearly unstable zones in the as-quenched or weakly stressed samples.

This empirical study thus leads to the emergence of a phenomenology of the non-affine shear response summarized in Section IV. While supporting the concept of shear transformation zones (STZ) or, equivalently, elastically loaded traps (SGR), it diverges from these models about two of their basic assumptions, namely independence of elementary events and the nature of noise. We think that it should be of use for further developments in the modelization of plasticity of amorphous media.

II. TRANSVERSE PARTICLE MOTION

A. 2D simulations in the AQS regime

We use here the same binary LJ mixture as that of ref.[4], namely large (L) and small(S) particle radii and numbers are: $r_L = 0.5$, $r_S = 0.3$, and $N_L = N_S(1 + \sqrt{5})/4$. These values ensure that no crystallization occurs at low temperature. Simple shear deformation is imposed using Lees-Edwards boundary conditions. We study systems of three different sizes $L \times L$, with $L = 10, 20, 40$.

The quasi-static regime corresponds to the limit where the external time scale $\dot{\gamma}^{-1}$ is much larger than that of internal relaxation processes. The system, starting from local equilibrium, thus follows adiabatically the shear-induced evolution of the corresponding energy minimum up to the spinodal limit where this minimum disappears and the system jumps into another local minimum of lower energy. The simulation proceeds as follows: a small increment δ of homogeneous shear strain is imposed, then energy is minimized using a conjugate gradient algorithm with a stringent convergence criterion (see [4] for details). We choose $\delta = 10^{-4}$, small enough to ensure that, for our system sizes, all elastic branches are well resolved. A

typical $\sigma(\gamma)$ curve is displayed on Figure 1.

Starting from an initial quench, we explore the shear range $\gamma \leq 2$. In order to characterize the stationary state, we only retain data for $\gamma > 0.1$, which ensures that initial transients are discarded, thus making details of the quenching protocol immaterial. We have been able to collect data on 100, 50 and 20 systems of respective sizes $L = 10, 20, 40$.

Following ref.[4], we make extensive use of the so-called non-affine tangent field $\{\mathbf{u_i}\}$, defined as the difference between the linear response of particle displacements to an increment of homogeneous strain and the corresponding homogeneous field. It is well-defined, and is computed, everywhere along each elastic branch.

B. Statistics of transverse displacements

In plastically deforming amorphous systems, non-affine displacement fields contain information about both, departures from standard continuum elastic behavior and the nature of plastic events. In our simple shear geometry, transverse particle displacements Δy_i are purely non-affine, while longitudinal ones mix affine and non-affine contributions. We thus focus on the normalized distributions $P(\Delta y, \Delta \gamma)$ of the Δy_i's for a fixed strain interval $\Delta \gamma$. The statistical ensemble is built by sampling, for all initial configurations, all the $\Delta y_i = y_i(\gamma_0 + \Delta \gamma) - y_i(\gamma_0)$ at each step γ_0 ($0.1 \leq \gamma_0 \leq 2 - \Delta \gamma$).

Our results agree qualitatively with those of Tanguy et al [10]. Namely (see Figure 2) $P(\Delta y, \delta)$ has a quasi-gaussian center and exhibits, beyond $\Delta y \sim 0.2$, an exponential tail. Its fine structure shows more clearly in the log-lin representation of the distribution $\tilde{P}(\zeta)$ of the scale variable $\zeta = \log(\Delta y)$. As displayed on Figure 3, for small strain intervals ($\Delta \gamma / \delta \sim$ a few units), the corresponding curves exhibit a peak at small Δy in the 10^{-4} range, together with a broad hump for larger values. As $\Delta \gamma$ increases, the peak shifts to the right and the hump amplitude grows, though without noticeable horizontal shift, until both merge, for $\Delta \gamma \approx 10^{-2}$.

Can we interpret this structure and its evolution in the light of the succession of elastic and plastic episodes which reflect into the sawtooth shape of the $\sigma(\gamma)$ response? Clearly, particle motion consists of a series of continuous trajectories interrupted by sudden jumps associated, respectively, with elastic episodes and plastic events. Since δ is our numerical strain resolution, each interval of length δ is, within our accuracy, defined as either purely

elastic or purely plastic. So, for $\Delta\gamma = \delta$, we can decompose P (and likewise $\tilde{P}$) as :

$$P(\Delta y, \delta) = \alpha_{pl}(\delta)\Pi_{pl}(\Delta y, \delta) + (1 - \alpha_{pl}(\delta))\Pi_{el}(\Delta y, \delta) \qquad (1)$$

where $\alpha_{pl}(\delta)$ is the fraction of "plastic intervals" in our ensemble, and Π_{pl} (resp. Π_{el}) are the normalized distributions associated with the plastic (resp. elastic) sub-ensemble. It now clearly appears (see Figure 4) that the small Δy behavior of $P(\Delta y, \delta)$ results entirely from elastic motion, while its hump and large-Δy tail are due to plastic events.

On this basis, we are now able to understand the evolution of $\tilde{P}$ with $\Delta\gamma$. We extend the above decomposition to $\Delta\gamma > \delta$, now defining as "plastic" any interval containing at least one plastic event. As $\Delta\gamma$ increases while remaining small with respect to the average length $(\delta\alpha_{pl}(\delta)^{-1}))$ of an elastic branch, most plastic intervals in general still contain only one plastic event, so that their fraction $\alpha_{pl}(\Delta\gamma) \approx (\Delta\gamma/\delta)\alpha_{pl}(\delta)$, while Π_{pl} remains quasi unchanged, because the scale of plastic slips is large compared with that of elastic ones. This explains the evolution (Figure 4) of the plastic hump which, as $\Delta\gamma$ increases, consists primarily in an upward shift with little change in shape.

In this regime, which corresponds to $\Delta\gamma/\delta << \alpha_{pl}(\delta)^{-1}$ (~ 100 for the 20×20 system), the fraction $\alpha_{el} = (1 - \alpha_{pl})$ of purely elastic intervals remains nearly constant (e.g., for $L = 20$ and $\Delta\gamma = 10\delta$, $\delta\alpha_{el}/\alpha_{el} \sim 0.1$), so that the variations with $\Delta\gamma$ of the elastic part of $\tilde{P}$, $\tilde{P}_{el} = \alpha_{el}(\Delta\gamma)\tilde{\Pi}_{el}$, directly reveal those of $\tilde{\Pi}_{el}$. Inspection of the numerical data suggests (see also Figure 4) that the rightward shifts of $\tilde{P}_{el}(\zeta)$ are roughly equal to $\log(\Delta\gamma)$. The plot (Figure 5) of $\tilde{P}_{el}$ *vs* $\log(\Delta y/\Delta\gamma))$ shows that the collapse is indeed excellent in the low and middle ranges of $(\Delta y/\Delta\gamma)$ values, but fails in the large Δy tails.

This collapse means that *during the purely elastic episodes separating plastic events non-affine displacements are essentially convective*: the γ-derivative of the y_i field is nearly constant over most of an elastic episode. This amounts to stating that the tangent non-affine field $\{\mathbf{u_i}\}$, although spatially disordered [11], remains quasi-quenched. Now, we know from ref. [14] that this cannot be true when the system comes close below a spinodal threshold γ_c. Indeed, in these near-critical regions, a gradually softening elastic mode develops, leading to a $(\gamma_c - \gamma)^{-1/2}$ divergence of $\{\mathbf{u_i}\}$. Clearly, it is the contribution of these near-critical softened configurations which explains the large-Δy tails of $\tilde{\Pi}_{el}$. The tail deflation (Figure 5) results from the fact that, as the interval $\Delta\gamma$ increases, the weight of these soft configurations is gradually transferred from $\tilde{\Pi}_{el}$ to $\tilde{\Pi}_{pl}$.

This analysis clarifies the physical significance of the shape of $P(\Delta y, \Delta\gamma)$ in the moderate $\Delta\gamma$ range (where its non-Gaussian parameter remains large [10]): *(i)* Its quasi-gaussian center [11] results from small-scale non-affine displacements accumulated along purely elastic segments, during which particle trajectories are essentially convected. *(ii)* Its quasi-exponential tail arises from plastic jumps during plastic events.

For larger $\Delta\gamma/\delta \gtrsim \alpha_{pl}(\delta)^{-1}$, however, the decomposition of equation (1) loses physical content since the statistical weight of elastic intervals vanishes while $\tilde{\Pi}_{pl}$ mixes both elastic and plastic contributions. In order to circumvent this limitation, we concentrate in the following on the evolution with $\Delta\gamma$ of the second moment $\langle \Delta y^2 \rangle$.

C.   Transverse particle diffusion

In order to elucidate the nature of the transverse particule dynamics, we have computed from our data the space and ensemble average $\langle \Delta y^2 \rangle$ for increasing values of $\Delta\gamma$. On Figure 6 we plot the effective diffusion coefficient $D(\Delta\gamma) = \langle \Delta y^2 \rangle / \Delta\gamma$. For our three system sizes, $D(\Delta\gamma)$ exhibits the same qualitative features, namely it increases from a finite value $D_0 = \lim_{\Delta\gamma \to 0} D$, and saturates at a finite value D_∞ for large $\Delta\gamma$ ($\gtrsim 0.5$). However, D is strikingly system-size dependent, $D^{(L)}(\Delta\gamma)$ increasing with L for all $\Delta\gamma$'s.

Again, in order to shed light on the origin of this behavior, let us separate explicitly the elastic and plastic contributions to non-affine particle motion. Indeed, we can write:

$$\frac{dy_i}{d\gamma} = u_{iy}(\gamma) + \sum_a Y_i^a \delta(\gamma - \gamma_a) \tag{2}$$

where a labels the strain values where irreversible events (avalanches) occur, so that :

$$D(\Delta\gamma) = D_{ee}(\Delta\gamma) + D_{ep}(\Delta\gamma) + D_{pp}(\Delta\gamma) \tag{3}$$

with

$$D_{ee}(\Delta\gamma) = \frac{1}{\Delta\gamma} \left\langle \int_{\gamma_0}^{\gamma_0 + \Delta\gamma} d\gamma \int_{\gamma_0}^{\gamma_0 + \Delta\gamma} d\gamma' u_{iy}(\gamma) u_{iy}(\gamma') \right\rangle \tag{4}$$

and D_{ep}, D_{pp} the corresponding cross-correlated and plastic-plastic contributions. These three functions carry the information about self and cross correlations of elastic and plastic non-affine displacements.

Let us first consider the $\Delta\gamma \to 0$ limit. A straightforward asymptotic analysis taking into account the square-root divergence of the tangent field $\{\mathbf{u_i}(\gamma)\}$ at spinodal points leads to:

$$D_{ep}(\Delta\gamma) = \mathcal{O}(\Delta\gamma^{1/2}) \tag{5}$$

$$D_{ee}(\Delta\gamma) = \mathcal{O}\left(-\Delta\gamma\,\mathrm{Log}(\Delta\gamma)\right) \tag{6}$$

So, their contribution to $D(\Delta\gamma)$ vanishes, and the finite value of D_0 originates only from avalanches:

$$D_0 = \lim_{\Delta\gamma\to 0} D_{pp} = f\left\langle (Y_i^a)^2 \right\rangle \tag{7}$$

with

$$f = \lim_{\delta\to 0}\left[\frac{\alpha_{pl}(\delta)}{\delta}\right] \tag{8}$$

the average avalanche frequency, and $\langle (Y_i^a)^2 \rangle$ the variance of transverse displacements in a single plastic event.

It was shown in [4, 13] that f increases with size roughly as the lateral system size L. Using the measured frequency, we find that the variance $\langle (Y_i^a)^2 \rangle = D_0 f^{-1}$ decreases slowly with size: for $L = 10, 20, 40$, we get $10^4\langle (Y_i^a)^2 \rangle = 37, 26, 20$. We will come back to this point later.

Figure 7 shows the decomposition (eq.(3)) for $L = 20$. It is seen that, for all $\Delta\gamma$, D_{pp} remains the dominant contribution. $D_{pp}(\Delta\gamma)$ grows, then saturates. Its growth range $\Gamma_{pp} \sim 0.25$ shows no clear size dependence. This behavior entails that plastic events are correlated over a finite $\Delta\gamma$ range, which we understand as measuring a typical shear range over which the structural features involved in plastic events retain their identity.

For all sizes, $D_{ep}(\Delta\gamma)$, though much smaller than D_{pp}, exhibits an analogous behavior with a similar correlation range. This indicates that the above-mentioned persistent structures dominate the non-affine elastic response. Moreover the near square-root behavior [15] of D_{ep} for small $\Delta\gamma$ signals that the field $\{\mathbf{u_i}\}$ in a given near-critical region is strongly correlated with the displacements associated with the subsequent avalanche.

Finally, D_{ee} also rises and saturates, but more slowly than D_{ep} and D_{pp}. From the data for the three system sizes, we evaluate its correlation range to be $\Gamma_{ee} \sim 1$. That is, a single renewal, after $\Delta\gamma \sim \Gamma_{pp}$, of the "active structures" is not sufficient for the non-affine field to fully decorrelate. This we take as a hint of the fact that active structures occupy on average a fraction only of the total system "volume". With this interpretation, we evaluate this fraction as $\Gamma_{pp}/\Gamma_{ee} \sim 1/4$.

III. ZONE EMERGENCE, FLIPS AND ELASTIC COUPLINGS

Two phenomenological models of plasticity of jammed disordered media – namely the STZ theory of Falk and Langer [9, 16], and the soft glass rheology (SGR) of Sollich et al [17, 18] – have been proposed recently. Both describe, explicitly (STZ) or implicitly (SGR), plastic events as transitions concerning small regions, modelized as either Eshelby-like transformations or jumps out of traps in the energy landscape. These flips are viewed as independent, hence individual, and governed by the combined effect of external drive and of a thermal-like noise.

A question then immediately arises : are our above results consistent with the basic ingredients of these models? We now try to answer it by careful inspection of the evolution of the spatial structure of the non-affine tangent field $\{\mathbf{u_i}\}$.

A.   Identification of active structures

Let us first recall that $\{\mathbf{u_i}\}$ can be written as [14]:

$$u_{i\alpha} = H^{-1}_{i\alpha,j\beta}\Xi_{j\beta} \tag{9}$$

$$\Xi_{j\beta} = -\frac{\partial^2 U}{\partial\gamma\partial r_{j\beta}} \tag{10}$$

where (i, j) label particles and (α, β) cartesian components. U is the total energy of the LJ system, and $\bar{\bar{H}}$ the associated hessian matrix. $\Xi\delta\gamma$ is the field of particle force increments generated by an infinitesimal increment of homogeneous shear. $\{\mathbf{u_i}\}$ can be decomposed on the eigenmodes $\boldsymbol{\Psi_n}$ of $\bar{\bar{H}}$ (the phonon modes). Upon approaching a spinodal point, a single one, $\boldsymbol{\Psi_1}$, softens critically [14, 19]. So, in near critical regions, $\{\mathbf{u_i}\}$ exhibits a square-root divergence and is dominated by its projection $\mathbf{u_1}$ on $\boldsymbol{\Psi_1}$. This property enables us to clearly characterize the active structures close to the onset of plastic events.

The features we identify as characteristic of the evolution of $\{\mathbf{u}\}$ are exemplified on Figures 8 and 9. In these figures, for each value of γ we decompose the total non-affine field as:

$$\mathbf{u} = \mathbf{u_1} + \mathbf{u_2} + \tilde{\mathbf{u}} \tag{11}$$

with $\mathbf{u_{1,2}}$ its projections on the two modes $\boldsymbol{\Psi_{1,2}}$ with lowest eigenvalues $(\lambda_1 < \lambda_2)$.

9

We observe that, in all cases, the active structures emerge out of a quasi-random small background as one or several localized zones characterized by strong quadrupolar contributions to $\mathbf{u}$. These quadrupoles are approximately aligned with the principal directions of the homogeneous strain. As zones approach instability, they soften, and the corresponding growing part of $\mathbf{u}$ concentrates into the lowest mode component $\mathbf{u_1}$.

After identifying them in prespinodal regions, we are able to trace them *back* over sizeable γ-ranges before their amplitude has decreased enough for them to gradually merge into the global disordered background structures. In some cases, this range of visibility extends across one or more plastic events. A typical sequence illustrating this behavior, shown on Figure 8, extends over a range of $\Delta\gamma \sim 3\%$, to be compared with the average length $\Delta\gamma \sim 1\%$ of elastic episodes for this system size.

B. Zone flips

Each discontinuous drop on the $\sigma(\gamma)$ curve is associated with the sudden disappearance of one or more of these soft zones (Figures 8 and 9). Noticeably, the resulting changes in $\{\mathbf{u_i}\}$ remain quite localized, leaving most of the other prominent structures of the non-affine pattern essentially unchanged. In particular, zones which were already clearly visible are commonly seen to survive the plastic event (see Figure 8).

We have shown in Section II.2 that particle jumps $\{\Delta\mathbf{R_i^a}\}$ in plastic events are well correlated with the precritical $\{\mathbf{u_i}\}$ structure. This entails that the flip of a zone Z is associated primarily with a quadrupolar displacement field of finite amplitude centered on Z. This supports the representation, proposed by Argon and coworkers [3, 8] and explicited by Picard et al [7], of the elementary dissipative process as the Eshelby-like shear transformation of a self generated inclusion involving a few particles, which is also the basis of the STZ theory.

This representation is also consistent with the main features of the distribution $\Pi_{pl}(\Delta y, \delta)$ of particle displacements induced by plastic events (see § II.B). Indeed, the plot on Figure 10 shows that that Π_{pl} becomes exponential for $\Delta y \gtrsim 0.2$. In the Eshelby picture, we expect large Δy to correspond to displacements within the transforming zone(s), while smaller Δy are associated with particles sitting in the surrounding elastic medium. In this picture, we interpret the exponential tail of Π_{el}, hence of the full distribution P, as reflecting the

diversity of intrazone structures. We thus expect that, upon varying the system size, the logarithmic slope of the tail should remain constant. As shown on Figure 10, this prediction is very nicely verified for our three L values. Moreover, it appears that the tail amplitude decreases with increasing L. In our interpretation, the statistical weight of the exponential tail is controlled by the volume fraction of zone cores involved in plastic events. Since the average size of the avalanches constituting plastic events scales roughly as L, we expect the corresponding core volume fraction to decrease with size, in agreement with the observed behavior.

So, we interpret the existence of an exponential tail in $P(\Delta y)$ as a consequence of structural disorder within transforming zones, and by no means as a signature of avalanche behavior, which only affects the tail amplitude.

C.   Elastic couplings

Consider the sequence shown on Figure 9. For $\gamma = 0.1150$ (Figure 9-a) two zones are clearly discernible in the $\mathbf{u}$ pattern. At $\gamma = 0.1160$ (Figure 9-b) their amplitude has grown, and they appear in the projection $\mathbf{u_2}$ of $\mathbf{u}$ on the next-to-lowest mode. At $\gamma = 0.1161$ (Figure 9-c) they are slightly softer and have invaded the projection $\mathbf{u_1}$ on the lowest mode. Note that, in these last two cases, they appear in the non-trivial soft mode as connected by "flow lines" which reproduce the most prominent vortex structures first described by Tanguy et al [20]. This is particularly clear when two relatively distant zones soften simultaneously as shown on Figure 11.

From these and many similar observations (see Figure 8) we deduce that :

• Soft zones are coupled elastically via their quadrupolar fields.

• It is the associated flow lines which form the conspicuous vortex-like patterns characteristic of non-affine fields in amorphous solids. That such patterns are akin to incompressible flows results from the fact that these systems are much more compliant in shear than in compression. For our 2D LJ glass [4]: $\mu = 39$, $K = 236$.

Quadrupolar couplings result, in the homogeneous elastic continuum approximation for the background medium, from a stress field $\sim \cos(4\theta)/R^2$ (with R the length and θ the orientation with respect to $\hat{x}$ of the interzone vector). Notice that, in Figure 9, in $\mathbf{u_1}$ the fields of the two zones Z_1, Z_2, which are quasi vertically aligned, combine positively.

We have checked that, in consistence with the above remark, zone pairs lying in sectors corresponding to negative couplings combine negatively in the phonons $\mathbf{\Psi_1}$ and $\mathbf{\Psi_2}$: in this case, one of the two zones appears with an opposite sign, i.e. with reversed flow lines. These observations confirm the relevance of inter-zone elastic couplings.

It is intuitively clear that configurations with strongly coupled soft zones are good candidates for simultaneous flips, as illustrated on Figure 8 and 9. We observe a number of multi-zone flips, involving the disappearance of at least one diverging quadrupole, as well as that of some less visible zones. Moreover, plastic events alter the amplitude of the near-critical surviving zones in $\mathbf{u}$ (see Figure 8) in a way which appears roughly consistent with quadrupolar couplings.

IV. A PHENOMENOLOGY OF SHEAR ZONES

The various pieces of information which we have gathered and presented above can now be organized into a rather detailed phenomenology of plasticity in our system in the AQS regime, which can be schematized as follows.

(i) Structural disorder gives rise, in such a glassy system, to the existence of strong inhomogeneities, or zones. These zones can be viewed as small inclusions à la Eshelby, embedded in a quasi-homogeneous elastic background, and plastically transformable under shear. They are advected by external shear toward their instability threshold. Upon approaching it, a zone softens, then flips at its spinodal and disappears.

The correlation range Γ_{pp} between plastic events (see Section II.2) provides an evaluation of the amount of strain necessary to fully renew the population of zones. Here $\Gamma_{pp} \sim 0.25$.

One renewal is not sufficient, however to decorrelate fully the non affine field. This suggests that zones occupy a fraction only of the system, of order Γ_{pp}/Γ_{ee}, here $\sim 1/4$.

(ii) Zone elastic softening and plastic flipping are both associated with quadrupolar components in the non-affine displacement field which give rise to inter-zone elastic couplings. Due to the long range of elastic fields, a zone flip thus alters the local strain level at any other zone site in the system, the resulting γ-shift depending, in amplitude and sign, on the relative position of source and target. These signals have two types of effects.

— A flip signal may shift the strain level of some zones beyond their threshold γ_c, thus triggering their flip and initiating a cascade. In the QS regime, where acoustic delays are neglected, such cascades are instantaneous.

— For the non-flipping zones, the elastic signals resulting from flips constitute a dynamical noise, acting in parallel with the externally imposed advection, whose frequency scale is proportional to the strain rate $\dot{\gamma}$.

So, in agreement with the previous proposition of Bulatov and Argon [3, 8], also underlying recent models by Picard et al [21] and by Baret et al [22], we conclude that elastic couplings between zones play an essential role, by inducing avalanches and generating the dominant contribution to the disorder-induced noise. At $T = 0$ and moderate strain rates, it is this dynamical elastic noise which, in addition to strain advection, must appear in models of plasticity of jammed media. In a forthcoming article, we will propose such a schematic model, and show that it accounts for a system-size scaling behavior of avalanches.

Within the foregoing picture, we interpret the two kind of events invoked by Tanguy et al [10] as plastic events of different sizes. Namely, their transient shear bands exhibit the characteristics expected for large avalanches of the type described above, their directionality resulting from that of quadrupolar couplings in their system with two rigid walls. Their local events correspond to the small stress drops appearing during initial transients (see Figure 1): at low stress levels, before advection has been able to significantly feed the near-threshold population, we indeed understand that avalanche triggering is unlikely, hence that single flip events are the rule.

Let us finally stress that the above zone phenomenology remains very schematic. Indeed, exhaustive inspection of the evolution of **u** reveals that zone life is somewhat more eventful than our simplified description suggests. Rather frequently, we see a given zone undergoing a few flips before it disappears. Such zones can be termed multi-state. In other instances, a barely visible zone emerges fast enough to "overtake" previously more visible, softer, ones. That is, zone moduli and, very likely, thresholds are not unique, but distributed about an average. These remarks point toward the interest of pursuing extensive characterization of elastic heterogeneity in jammed systems, in particular via studies of coarse grained elastic moduli.

On a more speculative level, we would like to raise an important question: are the irreversible transformations identified here under shear related to the dynamic hetero-geneities [23, 24, 25, 26] characteristic of glassy dynamics near and below T_g? Indeed, we share the opinion, formulated long ago by Goldstein [27], that at finite temperature "re-arrangements are of course occurring all the time in the absence of an external stress; the external stress, by biasing them, reveals their existence".

Our active zones are primarily sensitive to shear. This, we think, must be put together with recent results by Widmer-Cooper and Harrowell [28, 29]. These authors show that dynamic propensity in a 2D LJ glass is uncorrelated with free volume, which we understand to mean that their local rearranging structures are only wekly coupled to compression. This leads us to suggest that their observation that zones of high propensity have large "Debye-Waller factors" amounts to identifying them as soft zones sensitive to shear – a speculation which will demand extensive future investigation.

---

[1] S. Kobayashi, K. Maeda, and S. Takeuchi, Acta Met **28**, 1641 (1980).

[2] D. Deng, A. S. Argon, and S. Yip, Philos. Trans. R. Soc. Lond. Ser. A-Math. Phys. Eng. Sci. **329**, 549 (1989).

[3] A. S. Argon, V. V. Bulatov, P. H. Mott, and U. W. Suter, J. Rheol. **39**, 377 (1995).

[4] C. Maloney and A. Lemaître, Phys. Rev. E **74**, 016118 (2006).

[5] N. Bailey, J. Schiøtz, A. Lemaître, and K. Jakobsen, Phys. Rev. Lett. **98**, 095501 (2007).

[6] J. D. Eshelby, Proc. Roy. Soc. London A **241**, 376 (1957).

[7] G. Picard, A. Ajdari, F. Lequeux, and L. Bocquet, Eur. Phys. J. E **15**, 371 (2004).

[8] V. V. Bulatov and A. S. Argon, Model. Simul. Mater. Sci. Eng. **2**, 167 (1994).

[9] M. L. Falk and J. S. Langer, Phys. Rev. E **57**, 7192 (1998).

[10] A. Tanguy, F. Leonforte, and J.-L. Barrat, cond-mat/0605397, 2006.

[11] Note that the position of the peak of $\tilde{\Pi}_{el}$ corresponds, roughly, to the width of the gaussian approximant of the small-Δy part of $P(y, \delta)$.

[12] M. J. Demkowicz and A. S. Argon, Physical Review B **72**, 245206 (2005).

[13] C. Maloney and A. Lemaître, Phys. Rev. Lett. **93**, 16001 (2004).

[14] C. Maloney and A. Lemaître, Phys. Rev. Lett. **93**, 195501 (2004).

[15] Strictly speaking, in order to observe the asymptotic $\Delta\gamma^{1/2}$ behavior, we would need data for decreasing simulation strain intervals $\delta \to 0$. With our value $\delta = 10^{-4}$, we measure at small $\Delta\gamma$ an effective behavior $D_{ep} \sim \Delta\gamma^{0.6}$.

[16] M. L. Falk and J. S. Langer, M.R.S. Bulletin **25**, 40 (2000).

[17] P. Sollich, F. Lequeux, P. Hébraud, and M. E. Cates, Phys. Rev. Lett. **78**, 2020 (1997).

[18] P. Sollich, Phys. Rev. E **58**, 738 (1998).

[19] D. L. Malandro and D. J. Lacks, J. Chem. Phys. **110**, 4593 (1999).

[20] A. Tanguy, J. P. Wittmer, F. Leonforte, and J.-L. Barrat, Phys. Rev. B **66**, 174205 (2002).

[21] G. Picard, A. Ajdari, F. Lequeux, and L. Bocquet, Phy. Rev. E **71**, 010501 (2005).

[22] J. C. Baret, D. Vandembroucq, and S. Roux, Phys. Rev. Lett. **89**, 195506 (2002).

[23] B. Doliwa and A. Heuer, Physical Review E **67**, 031506 (2003).

[24] B. Doliwa and A. Heuer, Physical Review E **67**, 030501 (2003).

[25] B. Doliwa and A. Heuer, Physical Review Letters **91**, 235501 (2003).

[26] T. B. Schrøder, S. Sastry, J. C. Dyre, and S. C. Glotzer, jcp **112**, 9834 (2000).

[27] M. Goldstein, J. Chem. Phys. **51**, 3728 (1969).

[28] A. Widmer-Cooper and P. Harrowell, Journal of Physics: Condensed Matter **17**, S4025 (2005).

[29] A. Widmer-Cooper and P. Harrowell, Physical Review Letters **96**, 185701 (2006).
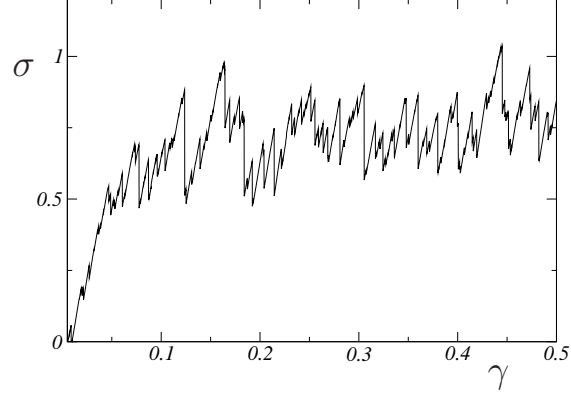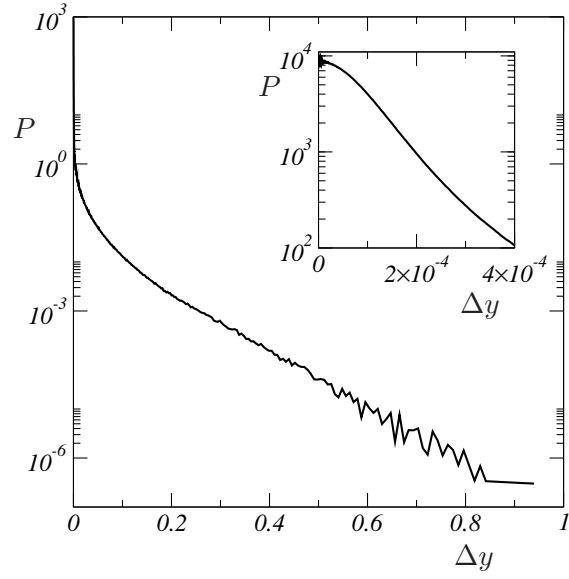
FIG. 1: Stress-strain curve for a 20×20 system.

FIG. 2: The distribution $P(\Delta y, \delta)$ of transverse particle displacements for the elementary strain step δ and for system size $L = 20$. Insert: Blow-up of the small Δy region.
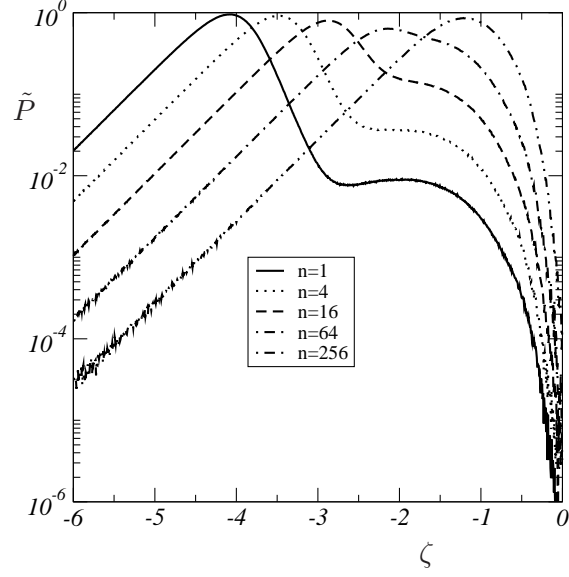
FIG. 3: The distribution $\tilde{P}(\zeta; \Delta\gamma)$ of the scale variable $\zeta = \log(\Delta y)$ for increasing values of $n = \Delta\gamma/\delta = 1, 4, 16, 64, 256$. System size: $L = 20$.
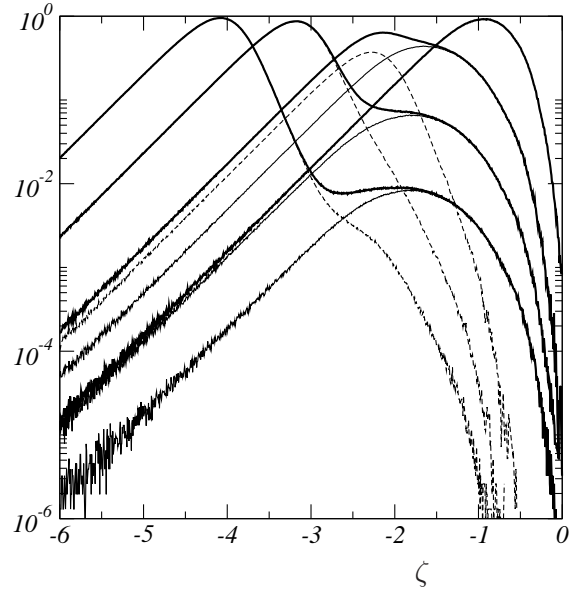

FIG. 4: Decomposition of the total distributions $\tilde{P}(\zeta; \Delta\gamma)$ (thick solid lines), for $n = \Delta\gamma/\delta = 1, 8, 64, 512$. For increasing n's, the maximum of the distribution shifts rightwards. Thin solid lines: contribution of plastic events; thin dashed lines: contribution of elastic branches (see text). System size $L = 20$.
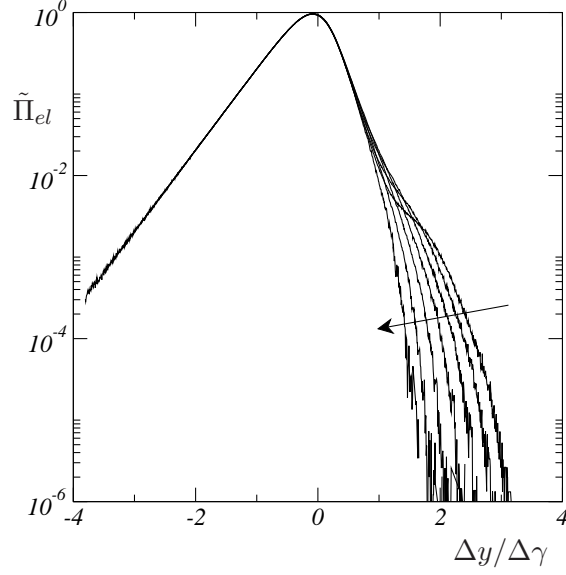
FIG. 5: The function $\tilde{\Pi}_{el}$ plotted versus $\Delta y/\Delta \gamma$ for $n = \Delta \gamma/\delta = 1, 2, 4, 8, 16, 32, 64$. The arrow indicates the direction of *increasing n*'s. System size $L = 20$.
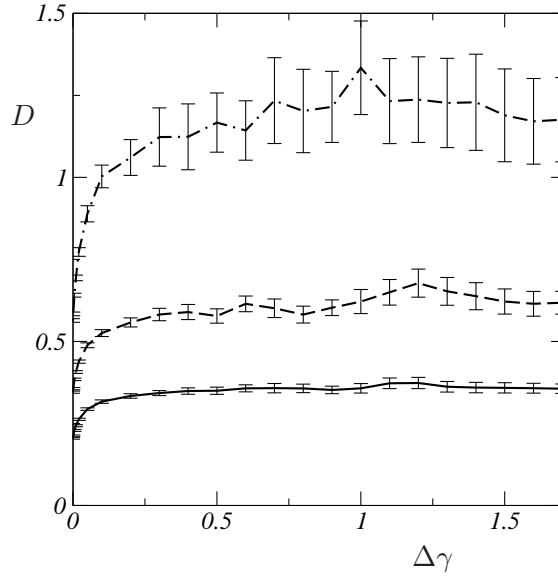
FIG. 6: From bottom to top: the instantaneous diffusion constant, $D(\Delta \gamma) = \langle \Delta y^2 \rangle/\Delta \gamma$ versus $\Delta \gamma$, for increasing system sizes $L = 10, 20, 40$ (and respectively 100, 50, and 20 samples). Error bars result from a standard Student analysis of the data.
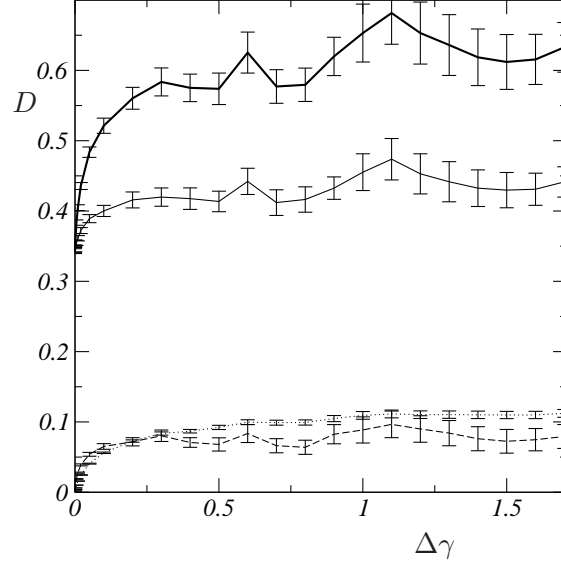
FIG. 7: The instantaneous diffusion constant, $D(\Delta\gamma) = \langle \Delta y^2 \rangle / \Delta\gamma$ for system size $L = 20$ (thick solid line) and its decomposition into D_{ee} (dotted line), D_{ep} (dashed line) and D_{pp} (thin solid line).
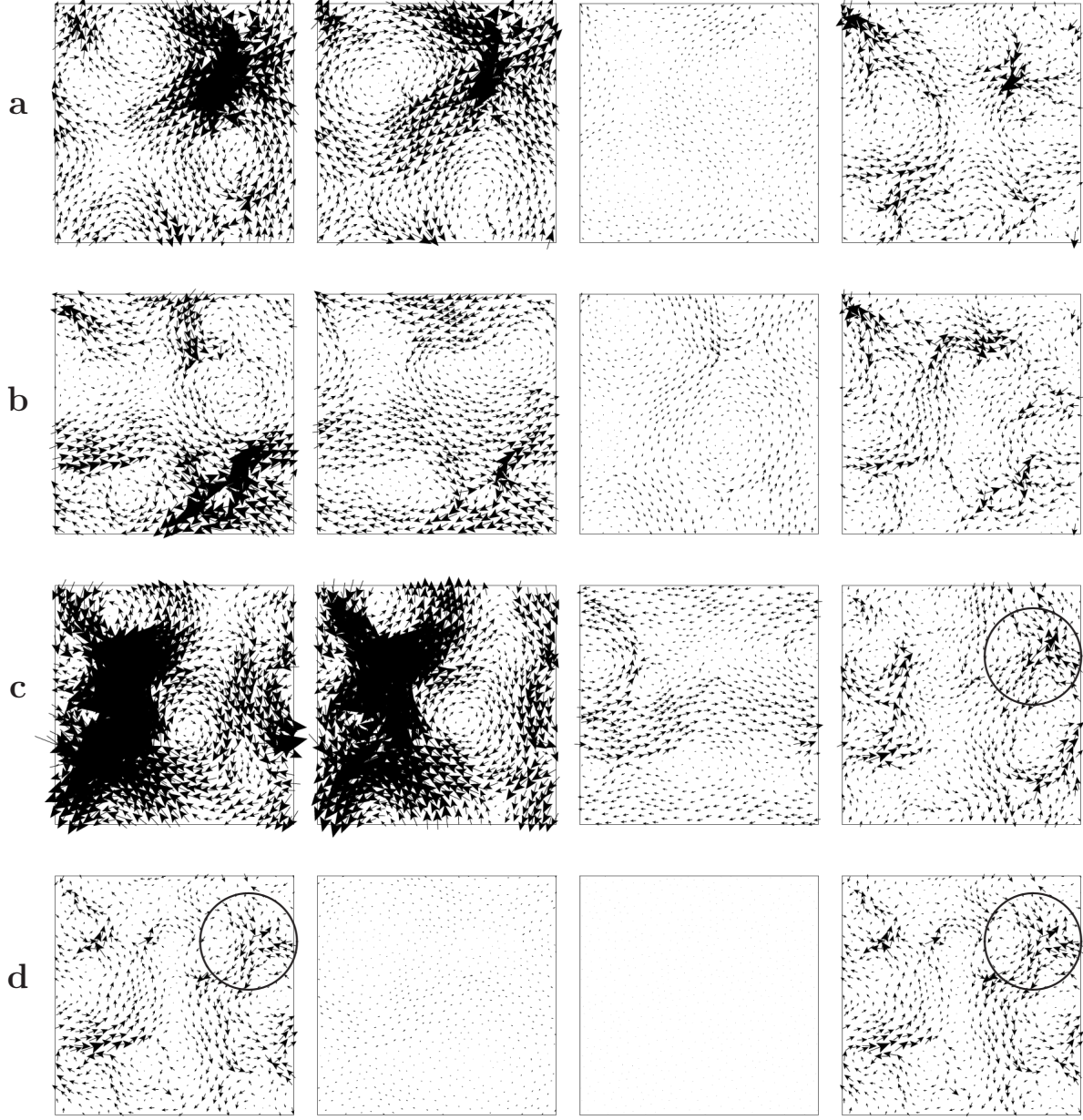
FIG. 8: System size: $L = 20$. Each line corresponds to a single strain value γ. The four frames present, from left to right, the non-affine tangent field $\mathbf{u}$ and its three components $\mathbf{u_1}$, $\mathbf{u_2}$, $\mathbf{\tilde{u}}$ as defined by equation (11).

(a): $\gamma = 0.0556$: a quadrupole, clearly visible in the upper right corner of both $\mathbf{u}$ and the soft mode component $\mathbf{u_1}$, signals a near-critical zone Z, which flips at $\gamma_c \in [0.0557, 0.0558]$.

(b): $\gamma = 0.0558$: Z has just flipped and disappeared, pushing another zone Z' (lowest right corners of $\mathbf{u}$ and $\mathbf{u_1}$) closer to its threshold. Note that Z' was already discernable (line a) in both $\mathbf{u}$ and $\mathbf{\tilde{u}}$ before the event.

20

(c-d): Zone Z, now indicated by circles, can be traced *back* to $\gamma = 0.0269$ (line c, frame $\mathbf{\tilde{u}}$). It
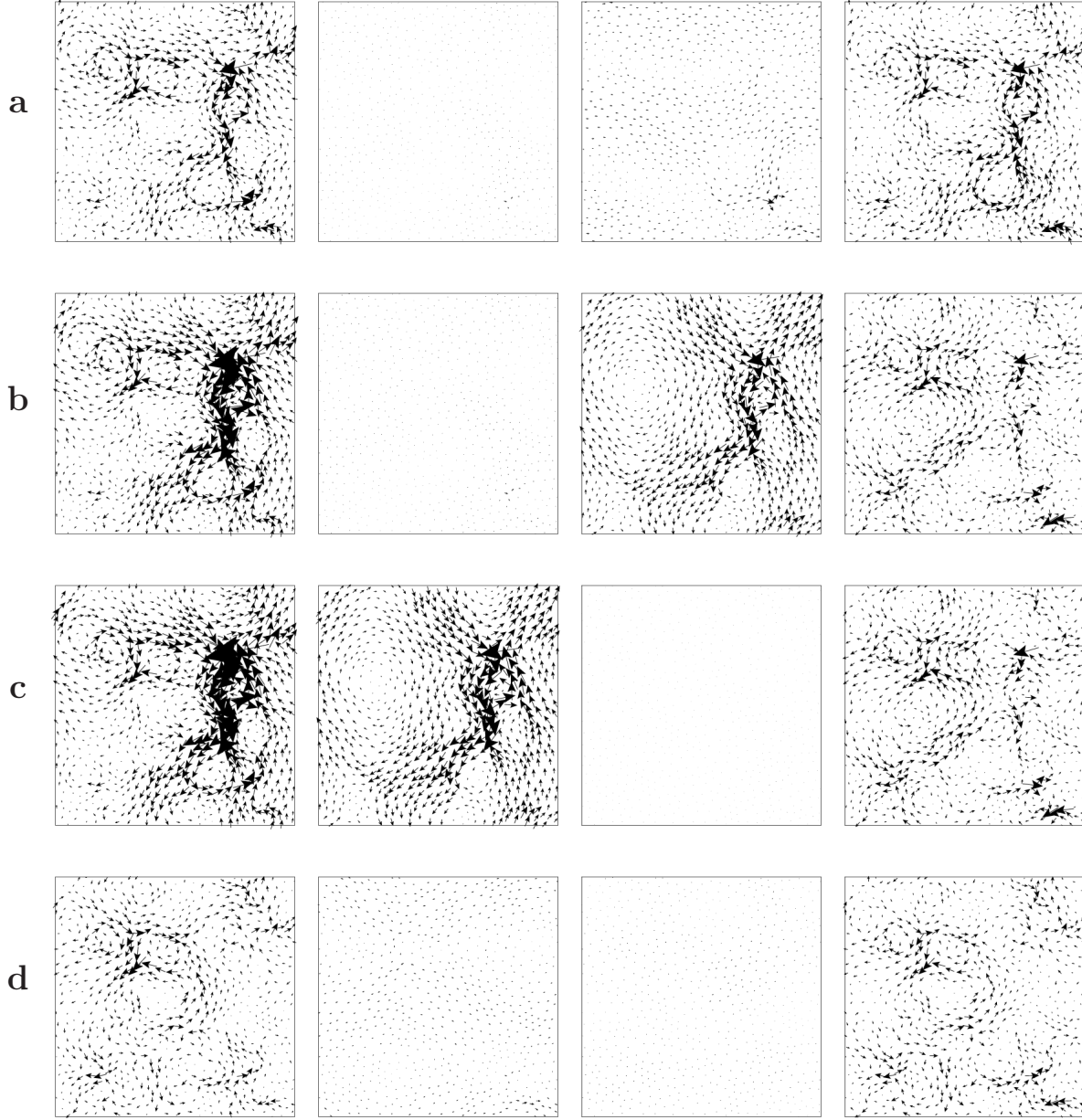
FIG. 9: From a to d: $\gamma = 0.1150$, 0.1160, 0.1161, and 0.1166. Two vertically aligned zones flip together in the interval $0.01165-66$ and disappear. As strain increases from $\gamma = 0.1150$, they soften and sequentially appear in $\mathbf{u_2}$, then in $\mathbf{u_1}$ after a clear level crossing in the interval $0.01160-61$. The connecting flow lines are a signature of their elastic coupling.
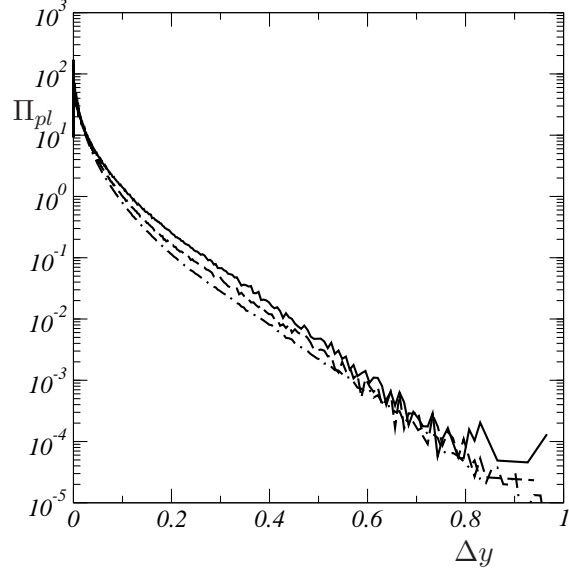
FIG. 10: The distribution $\Pi_{pl}(\Delta y, \delta)$ of particle displacements induced by plastic events for $L = 10, 20, 40$.
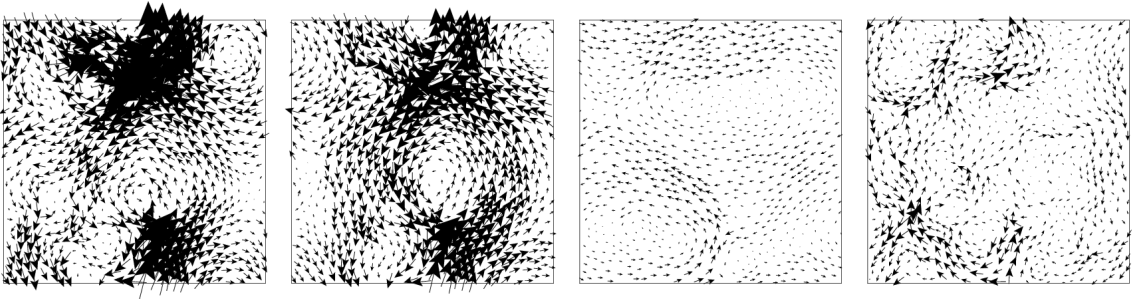

FIG. 11: Two distant zones soften simultaneously and appear in $\mathbf{u_1}$. The characteristic vortex-like structure signals their elastic coupling.